International Journal of ChemTech Research
CODEN (USA): IJCRGG ISSN: 0974-4290
Vol.8, No.11 pp 277-286, 2015

Optimization of sliding wear parameters of nano graphite reinforced Al6061-10TiB$_2$ hybrid composite using response surface methodology

C. M. Anand partheeban[1]*, M. Rajendran[2], and P.Kothandaraman[3]

[1]Research scholar, Anna university, Chennai, India.
[2]Department of Mechanical Engineering, KGISL Institute of Technology, Coimbatore, India.
[3] A.C.T. College of Engineering and Technology, Kancheepuram, India.

Abstract: This paper aims to optimize the wear parameter of Al6061-10TiB$_2$ composite, Al6061-10TiB$_2$-2Gr and Al6061-10TiB$_2$-4Gr nano hybrid composite using powder metallurgy method. The dry sliding wear test was performed using pin-on-disc equipment under atmospheric conditions, with the varying parameters of the applied load (5 -15*N*) and Sliding distance (1000 -3000 *m*) and the sliding velocity is kept constant of 2.61 *m/s*. The optimum parameters of wear and friction were identified using Response Surface Methodology and some useful conclusions were made.
Keywords: Aluminium hybrid composites, wear, coefficient of friction, optimization.

Introduction

Aluminum-based particulate reinforced Metal Matrix Composites (MMCs) has been receiving worldwide attention on account of high performance materials known for light weight, superior strength and stiffness. They find application in aerospace, automobile, marine, chemical, transportation, and mineral processing industries [1, 2]. Normally aluminium MMCs are manufactured by liquid state, semisolid and Powder Metallurgy (P/M) methods [3-8]. Among the manufacturing techniques of MMC, P/M method is a low cost method, suitable for high volume production of complicated shapes. It is widely used for the manufacturing of aluminium based composite materials [9]. The advantages are simplicity, flexibility and applicability to a large quantity production [10]. One of the main advantages of P/M when compared to casting is having better control on the microstructure and better distribution of the reinforcement is possible in P/M compacts [11-12]. The reinforcement materials are embedded into the matrix in the hybrid composite [13], which is characterized by light weight, high strength, high stiffness, good toughness and desired wear resistance than those of conventional materials [14]. Aluminium-graphite particulate MMCs produced by P/M techniques represent a class of inexpensive tailor-made materials for a variety of engineering applications such as automotive components [15], bushes and bearings [16]. Because of this solid lubricate property, graphite in the form of particles has a wide range of applications in composite materials. They are used to make components requiring tensile, and great wear resistance such as engine bearing, pistons, piston rings and cylinder liners [17].

The wear resistance is an important factor for various engineering applications. Although the friction and wear properties of several aluminium alloys in unlubricated conditions are widely investigated, the additions of TiB$_2$ and Gr with Al6061 composites have been limited in tensile, hardness and wear [18]. Literatures confirm that only limited work is done on the sliding wear behavior of composite with TiB$_2$ as reinforcement material produced in situ [19]. The fundamental wear properties of ceramics like Al_2O_3, Si_3N_4, ZrO_2 and SiC in various contact situations showed that in mild wear [20]. The effect of sliding velocity on the tribological characteristics of Al-B_4C and Al-SiC MMCs against a commercial brake pad, it confirms that the weight loss increases with increasing the sliding velocity [21]. It was observed that higher sliding velocity led to lower wear rate and lower friction coefficient for both MMCs [22].

The wear results were optimized by Response Surface Methodology (RSM); in this, the relationship between the input and output variables for an experiment can be determined by using some modelling techniques. RSM is a blending of statistical and mathematical model tools for developing and optimizing the process parameters [23]. RSM has become a common practice in engineering problems, and it has been used extensively in characterization of the problems, in which the input variables influence some performance over the output variables. RSM provides quantitative measurements of possible interactions between factors, which are difficult to obtain using other optimization techniques. The authors have investigated the application of RSM for the optimization of the process characteristics [24]. RSM is the right procedure to deal with the responses influenced by multi-variables. This method significantly reduces the number of trials that are required to respond to a model [25].

Even though many researchers attempted Al6061 with TiB2 and Gr, literatures confirm that no work is done on optimization of wear paranters of Al6061 with TiB_2 and nano Gr as reinforcement material produced in solid and liquid phase method. In this investigation optimization of various tribological parameters of Al6061 based hybrid composites were investigated.

Materials and methods

Materials

The materials used for the present study were Al6061, TiB_2 and Gr. The Al and the reinforcing ingredient of the as received TiB_2 powder has the particle size of 30-50 μm and 1-10 μm, the graphite particle size varies from 25 μm to 50 μm.

Sample preparation

The Gr powder was pulverized into nano scale and mixed with TiB_2 and Al6061 powders using high energy ball mill (planetary mono mill, Fritsch, Germany-Pulverisette-6) with tungsten carbide vials using 10 mm diameter tungsten carbide balls. The ball to charge weight ratio was 20:1. Milling was done at 300 *rpm* in a wet medium, in the presence of toluene to prevent oxidation and agglomeration of the charges as explained in [11]. The Al6061 and hybrid composites of Al6061 were prepared by P/M method by adding 10 wt. % of TiB_2 and 2 & 4 wt. % of nano Gr after mechanical alloying. The mechanical alloying was performed for 2 hrs. During the mixing Al, TiB_2 and nano Gr were mixed in the same bowel. The cylindrical compacts were prepared from Al, TiB_2 and nano Gr powders using suitable punch and die set assembly on a Universal testing machine having 1 MN capacity. Compacting pressure was applied gradually and it was 1.2 GPa for all specimens [11]. Solid lubricant Gr was used to lubricate the punch, die and the butt. After the compaction, the compacts were immediately taken out from die set assembly and loaded into the furnace for sintering. To prevent oxidization, the green compacts were initially covered with inert argon atmosphere in the furnace.

The sintering was carried out in an inert gas circulated electric muffle furnace at 550°C for a holding period of one hour. As soon as the sintering schedule was over, the sintered preforms were cooled inside the furnace itself to the room temperature. After the completion of sintering the preforms were cleaned by using a fine wire brush. While preparing the compacts, the initial density of compact was 92% after sintering. The sintered preforms were extruded by the extrusion die set assembly as explained in [11-13]. The diameter of the specimen was reduced in different steps to get the density of extruded specimen as 99%. **Wear Test**

Dry sliding wear test was carried out using computerized wear testing pin-on-disc setup (Model: DUCOM, TR- 20LE- PHM- 400) in ASTM: G99 standards. All the experiments were conducted under atmospheric room conditions. During sliding, the load was applied on the specimen and it was brought in intimate contact with the rotating disc at track radius of 100 *mm*. Wear tests were carried out in the loads 5, 10 & 15 *N* at a constant sliding speed of 2.61 *m/s* and sliding distance of 1000, 2000 & 3000 *m* for each test.

During the testing the pin specimen was kept stationary and perpendicular to the disc while the circular disc was rotated. The initial weight of the specimen was calculated from a single pan electronic weighing machine with the precision of 0.0001 *g*. After each test, the counter face disk was cleaned with organic solvents to remove the traces. The coefficient of friction was computed from the recorded frictional force and applied load. The tribological behavior of Al6061-10TiB_2 composite, Al6061-10TiB_2-2Gr and Al6061-10TiB_2-4Gr nano hybrid composite was studied using the experimentally derived friction and the wear data.

Surface Response Methodology

The field of RSM consists of the experimental strategy for exploring the space of the process or independent variables and empirical statistical modelling, to develop an appropriate approximating relationship between the response and the process variables to develop empirical relationships to predict and optimize the wear rate and COF of the TiN coated surface. Important parameters that influence the specific wear rate and coefficient of friction were identified from literature. They are the % of nano Gr (A), Load (B), and sliding distance (C). For the selected input parameters, the second order polynomial regression equation used to represent the response surface 'Y' is given by ref. [29].

Wear rate =f (A, B, C) (1)
COF = f (A, B, C) (2)
$Y = b_0+\sum b_i x_i+\sum b_{ii} x_i^2+\sum b_{ij} x_i x_j + e_r$ (3)
And for the three factors, the selected polynomial could be expressed as
$SWR \text{ or } COF= b_0+b_1(A)+b_2(B)+b_3(C)+b_{11}(A^2)+b_{22}(B^2)+b_{33}(C^2)+b_{44}(D^2)+ b_{12}(AB)+b_{13}(AC) + b_{23}(BC)$ (4)

where b_0 is the average of the responses, and b_1, b_2. . . b_{23} are the coefficients that depend on the respective main and interaction effects of the parameters.

Results and discussion

Mathematical modelling and optimization

The results of the specific wear rate and COF are consolidated after the wear test, for the mathematical modelling and optimization through MINITAB 14 software. The experiment is designed according to the selected three factors with three levels, and it is given in Table 1 as explained in [25].

Table 1 Input levels of the wear parameters

S. No	Parameters	Low	Medium	High
A	Nano Gr (%)	0	2	4
B	Load (m/s)	5	10	15
C	Sliding distance (m)	1000	2000	3000

The RSM trials of the randomized design table are shown in Table 2. This table is plotted for "Three-level Full factorial L_{20}" using the Central Composite Design. It shows the response of the wear mass loss and COF, with respect to the independent factors such as % of nano Gr, load and sliding distance. The optimization is based on the "Smaller the best" concept, so that the parameters with the lowest wear rate and COF are considered as optimum. From this table, the counter graphs are plotted to identify the response; the plots are based on various combinations of the independent variables.

Table 2 Analytical table of responses for the independent variables

Trail	A	B	C	Wear Mass Loss (g)	COF
1	-1	1	1	0.00305	0.242
2	0	0	1	0.00278	0.484
3	1	-1	1	0.00227	0.513
4	1	1	1	0.00596	0.542
5	0	0	0	0.00204	0.515
6	0	0	0	0.00204	0.525
7	0	0	0	0.00208	0.514
8	1	-1	-1	0.00278	0.274
9	0	0	0	0.00268	0.455
10	0	-1	0	0.00212	0.553
11	0	0	-1	0.00284	0.456
12	0	1	0	0.00336	0.322
13	0	0	0	0.00204	0.515
14	-1	1	-1	0.00255	0.184
15	-1	-1	1	0.0029	0.138
16	1	1	-1	0.00395	0.438
17	0	0	0	0.00204	0.517
18	-1	-1	-1	0.00217	0.231
19	1	0	0	0.00212	0.417
20	-1	0	0	0.0031	0.475

Checking of data and adequacy of model

The normality of the data was assessed by means of the normal probability plot. The normal probability plot of the residuals for the wear mass loss and COF is shown in Fig. 1 (a) & (b) respectively. The normal probability plot for the wear mass loss and COF reveals that the residuals fall in a straight line. This means the errors are distributed normally. The Independence of the data was tested, by plotting a graph between the residuals, and the run order for a specific wear rate confirms that there was no predictable pattern observed, because all the run residues lay on or between the levels.

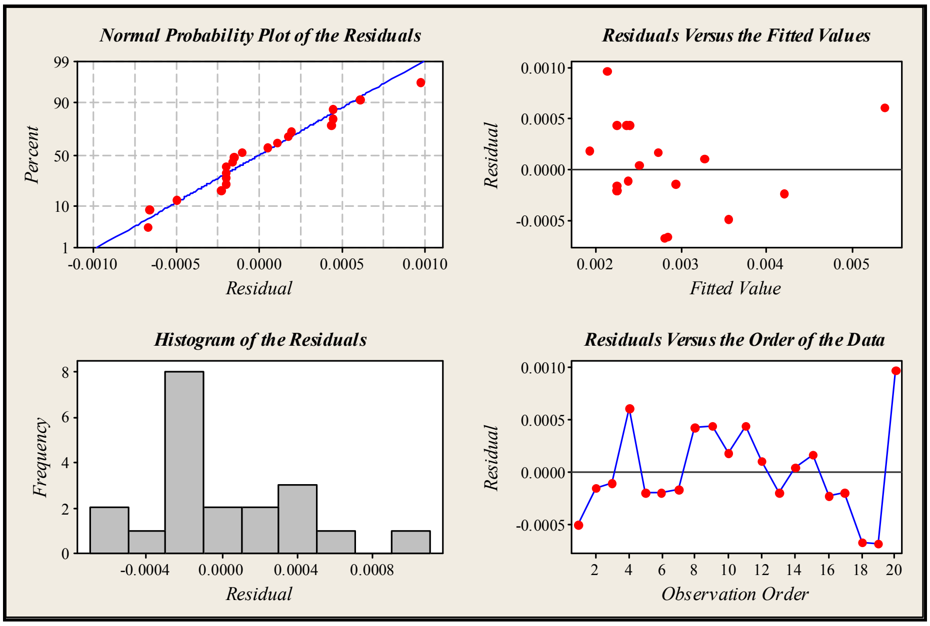

Fig. 1(a) Input data analysis plot for the specific wear rate

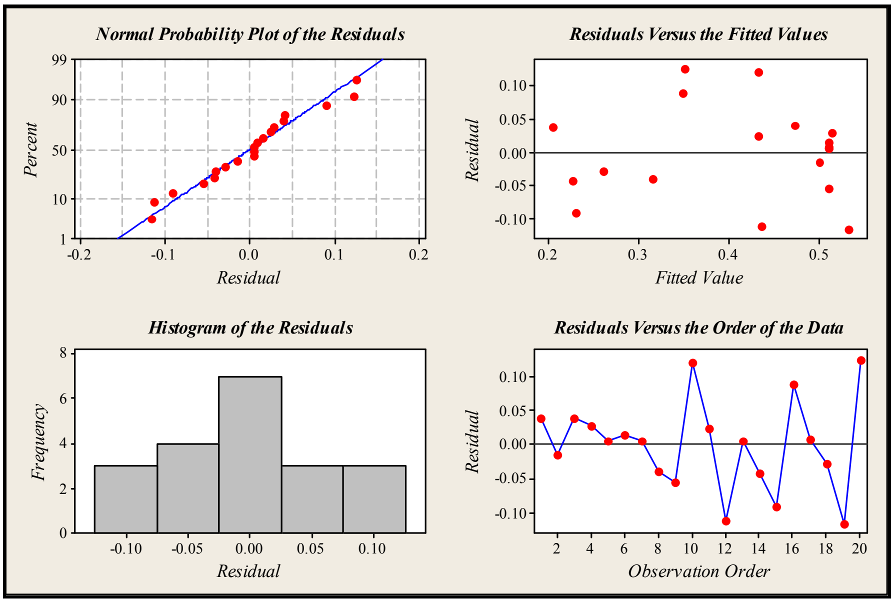

Fig. 1(b) Input data analysis plot for the COF

Estimated regression coefficients for the specific wear rate and COF

Table 3 shows the estimated regression coefficients for the wear mass loss. This table shows the wear mass loss of the possible influencing terms parameters discussed, and its effects are estimated. From the regression equation of wear mass loss (Equation 5), it was confirmed that the most influencing parameter for the wear mass loss is the % of nano Gr and load compared to distance. The significance of the developed model was tested, using the Analysis of Variance (ANOVA) technique. The determination coefficient (R^2) indicates the goodness of fit of the model [26]. In this case, the value of the determination coefficient (R^2 = 89.2%) indicates that only less than 5% of the total variance is not explained by the model. The value of the adjusted determination coefficient (adjusted R^2 = 80.5%) is also high, which indicates the high significance of the model.

Wear mass loss $_{est}$ = 0.00565591 - 6.29955E-04*A - 3.70514E-04*B - 2.02107E-06*C + 5.51136E-05*A*A + 1.40182E-05*B*B + 4.20455E-10*C*C + 5.41250E-05*A*B + 1.68750E-08*A*C + 5.72500E-08*B*C (5)

Table 3 Estimated regression coefficients for the wear mass loss

Term	Coef	SE Coef	T	P
Constant	0.002248	0.0002	11.257	0
Nano Gr	0.000331	0.000184	1.802	0.102
Load	0.000663	0.000184	3.61	0.005
Sliding distance	0.000267	0.000184	1.454	0.177
Nano Gr*Nano Gr	0.00022	0.00035	0.629	0.543
Load*Load	0.00035	0.00035	1.001	0.341
Sliding distance*Sliding distance	0.00042	0.00035	1.2	0.258
Nano Gr*Load	0.000541	0.000205	2.636	0.025
Nano Gr*Sliding distance	0.000034	0.000205	0.164	0.873
Load*Sliding distance	0.000286	0.000205	1.394	0.194

Table 4 shows the estimated regression coefficients for the COF. This table shows the COF of the possible influencing parameters discussed and its effects were estimated. From the regression equation of COF (Equation 6), it was inferred that the most influencing parameter in the COF is sliding distance, rather than the load and % of nano Gr. In this case, the value of the determination coefficient (R^2 =84.3%) indicates that only less than 5 % of the total variance is not explained by the model. The value of the adjusted determination coefficient (adjusted R^2 =81.1%) is also high, which indicates that the predicted R^2 is also in good agreement with the adjusted R^2.

$$COF_{est} = -0.0658091 + 0.0494045*A + 0.0573436*B + 0.000158168*C - 0.0169886*A*A - 0.00305818*B*B - 4.39545E-08*C*C + 0.00170000*A*B + 2.36250E-05*A*C + 4.00000E-07*B*C \quad (6)$$

Table 4 Estimated Regression Coefficients for COF

Term	Coef	SE Coef	T	P
Constant	0.509682	0.03176	16.048	0
Nano Gr	0.0914	0.02922	3.128	0.011
Load	0.0019	0.02922	0.065	0.949
Sliding distance	0.0336	0.02922	1.15	0.277
Nano Gr*Nano Gr	-0.06796	0.05571	-1.22	0.251
Load*Load	-0.07646	0.05571	-1.372	0.2
Sliding distance*Sliding distance	-0.04396	0.05571	-0.789	0.448
Nano Gr*Load	0.017	0.03266	0.52	0.614
Nano Gr*Sliding distance	0.04725	0.03266	1.447	0.179
Load*Sliding distance	0.002	0.03266	0.061	0.952

Interaction effect of the wear mass loss and COF

Fig. 2(a) shows the contour plots of the the wear mass loss corresponding to the input parameters, using Minitab. The various regions are used to identify the interaction effect with the help of changes in the contour plot. The interaction plot has been made for the % of nano Gr, load and sliding distance for the corresponding response value of the specific wear rate. It was inferred that the wear mass loss increases with the increase in Nano Gr (wt. %) and load. The maximum wear mass loss was identified at the maximum loading condition with 4 wt. % of nano Gr.

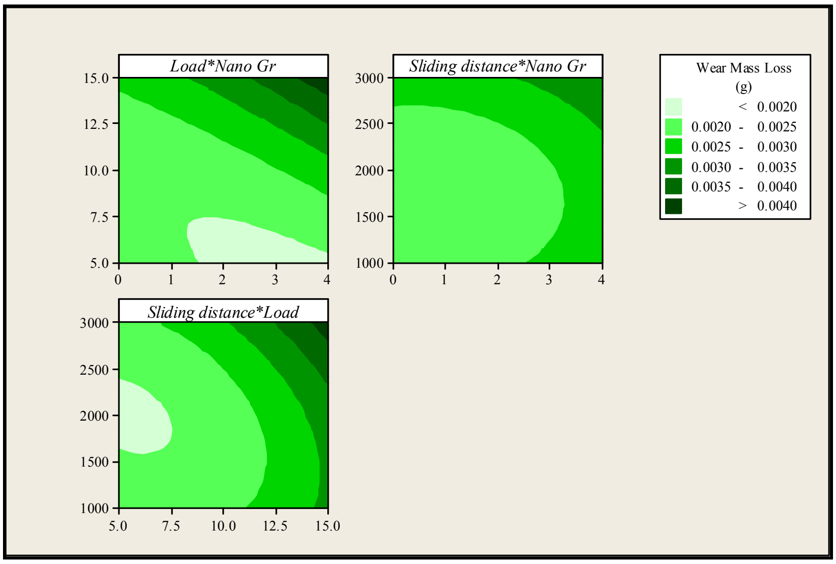

Fig. 2(a) Contour plots of the wear mass loss

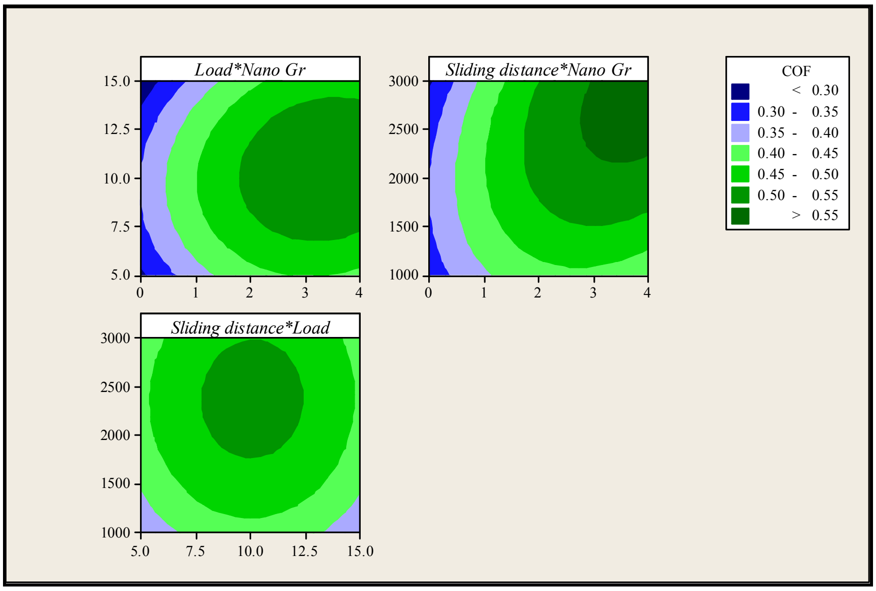

Fig. 2(b) Contour plots of COF

The 2D contour map of the COF is shown in Fig. 2(b). The various regions in the plot are easily identified with the help of changes in the colour of the contour plot. The plot was made between % of nano Gr, load and sliding distance for the corresponding response value of COF. The nano Gr influences much on COF compared to other parameters. The increase in nano Gr increases the COF with constant loading condition which was due to increase in reinforcement leads to three body mechanism.

ANOVA for the specific wear rate and COF

The ANOVA for the specific wear rate was done and tabulated in Table 5. From that, it was inferred that the p value is smaller than 0.5. It confirms that the developed model has 95 % confidence level, and we can use the developed model for future application [27]. Also, the P value is less (0.05) compared to the F value. It confirms that the developed models are adequate, and the predicted values are in good agreement with the measured data.

Table 5 Analysis of variance for the wear mass loss

Source	DF	Seq SS	Adj SS	Adj MS	F	P
Regression	9	0.000013	0.000013	0.000001	4.23	0.017
Linear	3	0.000006	0.000006	0.000002	6.13	0.012
Square	3	0.000004	0.000004	0.000001	3.6	0.054
Interaction	3	0.000003	0.000003	0.000001	2.97	0.083
Residual Error	10	0.000003	0.000003	0		
Lack-of-Fit	5	0.000003	0.000003	0.000001	9.1	0.015
Pure Error	5	0	0	0		
Total	19	0.000016				

The ANOVA result for the coefficient of friction is shown in Table 6, which indicates that the predictability of the model for COF is at 95% confidence level. The predicted response fits well with the experimentally obtained responses. A coefficient of determination shows that equation (7) is highly reliable. Further, the computed F value is greater than the p value, suggesting that the treatment is significant. Hence, the proposed model is a correct one. The ‘p’-value is less than 0.05, which indicates that the model is statistically significant.

Table 6 Analysis of variance for the COF

Source	DF	Seq SS	Adj SS	Adj MS	F	P
Regression	9	0.246303	0.246303	0.027367	3.21	0.042
Linear	3	0.094865	0.094865	0.031622	3.7	0.05
Square	3	0.131233	0.131233	0.043744	5.13	0.021
Interaction	3	0.020205	0.020205	0.006735	0.79	0.0527
Residual Error	10	0.085354	0.085354	0.008535		
Lack-of-Fit	5	0.08205	0.08205	0.01641	24.83	0.002
Pure Error	5	0.003305	0.003305	0.000661		
Total	19	0.331657				

Optimization

The optimal parameter of the wear mass loss and COF is to be confirmed from the results of the RSM fit plot (Fig. 3). The most influencing factors on wear mass loss and COF are load and nano Gr (wt. %) respectively. From Fig. 3, the optimal wear mass loss and COF are inferred from the plot 0.71978 which reveals that the optimal parameters are low load (5N) and high sliding distance (3000m) for the unreinforced composite. For the hybrid composite with 2 wt. % nano Gr obtained the minimum wear mass loss and COF at the same loading condition. The desirability for wear mass loss was 96.5% and 97.6% for COF with the composite desirability of 97.1%.

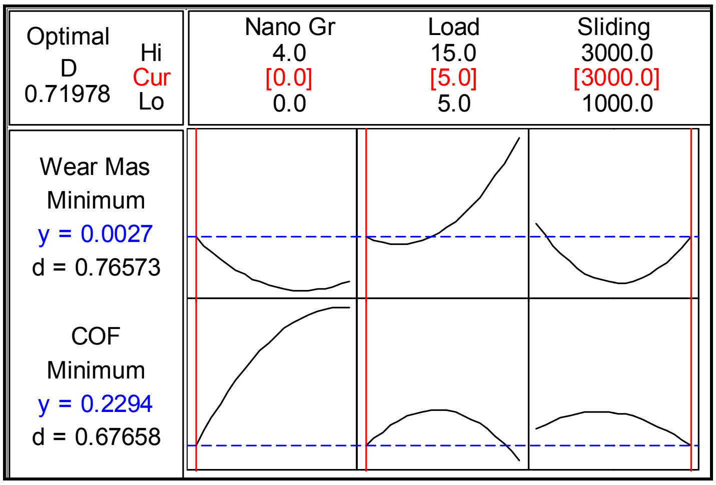

Fig. 3 Fit plot of the wear mass loss and COF

Conclusions

In this present research work, Al6061-10TiB_2 based composites and hybrid composites were prepared using P/M. The tribological behaviors such as wear and COF of the hybrid composite were carried out. Based on the present experimental and simulation work, the following conclusions are drawn:

- The hardness of the Al6061-TiB_2-Gr composite was increased mainly due to the weight percentage of the TiB_2 and Gr. The hardness increased with addition of reinforcements of TiB_2 & nano Gr with Al6061 matrix.
- For all the loads and the sliding distances, the developed hybrid composites have good wear resistance and coefficient of friction when compared with Al6061-10TiB_2 matrix. The addition of Gr reinforcement in Al6061-TiB_2 composites increased the wear resistance of the composites.
- From the regression analysis, it was inferred that the most influencing factors on wear mass loss and COF were load and nano Gr (wt. %) respectively.

- The optimal parameters were low load (5N) and high sliding distance (3000m) for the unreinforced composite and hybrid composite with 2 wt. % nano Gr for desirability level of 96.5% and 97.6% for wear mass loss and COF respectively with the composite desirability of 97.1%.

References

1. S. Lakshmi, L. Lu, M. Gupta, In situ preparation of TiB2 reinforced Al based composites, J. Mater. Process. Tech. 73 (1998) 160-166.
2. S. Natarajan, R. Naraynasamy, S.P. Kumaresh Babu, G. Dinesh, B. Anil kumar, K. Sivaprasad, Sliding wear behaviour of Al6063/TiB2 in situ composites at elevated temperatures, Mater. Des. 30 (2009) 2521-2531.
3. S. Suresh, N. Shenbaga Vinayaga Moorthi, Process development in stir casting and investigation on microstructures and wear behavior of TiB2 on Al6061 MMC, Proc. Eng. 64 (2013) 1183-1190.
4. R. Deaquino-Lara, E. Gutierrez-Castaneda, I. Estrada-Guel, G. Hinojosa-Ruiz, E. Garcia-Sanchez, J.M. Herrera-Ramirez, R. Perez-Bustamante, R. Martinez-Sanchez, Structural characterization of aluminium alloy 7075–graphite composites fabricated by mechanical alloying and hot extrusion, Mater. Des. 53 (2014) 1104-1111.
5. Vettivel S C., Ravi Kumar K. ffect of parameters on grinding forces and energy while grinding Al (A356)/SiC composites”, Tribology - Materials, Surfaces & Interfaces. 8 (2014) 235-240.
6. J. Hashim, L. Looney, M.S.J. Hashmi, Part 1, Particle distribution in cast metal matrix composites, J. Mater. Process. Technol. 123 (2002) 251-257.
7. C.S. Ramesh, AbrarAhamed, B.H. Chanabasappa, R. Keshavamurthy, Development of Al6063-TiB2 insitu composites, Mater. Des. 31 (2010) 2230-2236.
8. A. Ramesh, J.N. Prakash, A.S. Shiva Shankare Gowda, S. Appaiah, Comparison of the mechanical properties of Al6061/Albite and Al6061/Graphite metal matrix composites, J. Miner. Mater. Charact. Eng. 8(2) (2009) 93-106.
9. B. Ozge, A. Duygu, G. Hasan, D. Ismail, M. Lutfi Ovecoglu, Influence of TiB2 particle size on the microstructure and properties of Al matrix composites prepared via mechanical alloying and pressure less sintering, J. Alloys Compd. 586 (2014) 78-84.
10. N. Selvakumar, S.C. Vettivel. Thermal, electrical and wear behavior of sintered Cu–W nanocomposite. Mater Des 2013; 46: 16–25.
11. Selvakumar N, Mohan Raj AP, Narayanasamy R. Experimental investigation on workability and strain hardening behaviour of Fe–C–0.5Mn sintered composites, Mater Des 2012; 41:349–357.
12. S.C. Vettivel, N. Selvakumar, N. Leema, A. Haiter Lenin, Electrical resistivity, wear map and modelling of extruded tungsten reinforced copper composite, Mater. Des. 56 (2014) 791-806.
13. S.C. Tjong, K.F. Tam, Mechanical and thermal expansion behavior of hipped aluminum–TiB2 composites, Mater. Chem. Phys. 97 (2006) 91-97.
14. S. Suresh, N. Shenbaga Vinayaga Moorthi, S.C. Vettivel, N. Selvakumar, Mechanical behavior and wear prediction of stir cast Al-TiB2 composites using response surface methodology, Mater. Des. 59 (2014) 383-396.
15. C.S. Ramesh, S. Pramod, R. Keshavamurthy, A study on microstructure and mechanical properties of Al6061- TiB2 in-situ composites, Mater. Sci. Eng. A 528 (2011) 4125- 4132.
16. Baradeswaran A, Elaya Perumal A. Influence of B4C on the tribological and mechanical properties of Al7075-B4C composites, Compos. Part B 54 (2013) 146-152.
17. M. Roy, B. Venkatataraman, V.V. Bhanuprasad, Y.R. Mahajan, G. Sundararajan, The effect of particulate reinforcement on the sliding wear behavior of aluminium matrix composites, Metall. Mater. Trans. A 23 (1992) 2833- 2847.
18. S. Suresh, N. Shenbaga Vinayaga Moorthi, Aluminium-Titanium Diboride (Al-TiB2) Metal Matrix Composites: Challenges and Opportunities, Proc. Eng. 38 (2012) 89-97.
19. W. Weimin, F. Zhengyi, W. Hao, Runzhang, Influence of hot pressing sintering temperature and time on microstructure and mechanical properties of TiB2 ceramics, J. Eur. Ceram. Soc. 22 (2002) 1045-1049.
20. Pengting Li, Yunguo Li, Yuying Wu, Guolong Ma, Xiangfa Liu, Distribution of TiB2 particles and its effect on the mechanical properties of A390 alloy, Mater. Sci. Eng. A 546 (2012) 146-152.

21. S. Suresh, N. Shenbaga Vinayaga Moorthi, N. Selvakumar, S.C. Vettivel, Tribological, tensile and hardness behavior of TiB2 reinforced aluminium metal matrix composite" J. Bal. Tribol. Assoc. 20 (2014) 380-394.
22. B.P. Krishnan, N. Raman, K. Narayanaswamy, P.K. Rohatgi, Performance of Aluminium Alloy Graphite Bearings in a Diesel Engine, Tribol. Int. 16(5) (1983) 239-244.
23. Oraon B, Majumdar G, Ghosh B. Parametric optimization and prediction of electroless Ni–B deposition. Mater Des 28 (2007) 2138–47.
24. Saravanan I, Elaya Perumal A, Vettivel S C, Baradeswaran A. Optimizing wear behaviour of TiN coated SS 316L disc against Ti alloy using RSM, Mater Des 67 (2015) 469–4827.
25. Baradeswaran A, Elayaperumal A, Franklin I R. A Statistical Analysis of Optimization of Wear Behaviour of Al-Al 2 O 3 Composites Using Taguchi Technique. Procedia Engineering 64 (2013) 973-982.
26. Jinnah Sheik Mohamed M, Selvakumar N, Jeyasubramanian K, Vettivel S C. Numerical modelling on corrosion behaviour of molybdenum-based ceramic nanocomposite coated mild steel using response surface methodology. I J Surf Sci Engg 7 (2013) 345-365.
27. Baradeswaran A, Vettivel S C, Perumal A E, Selvakumar N, Issac R F. Experimental investigation on mechanical behaviour, modelling and optimization of wear parameters of B 4 C and graphite reinforced aluminium hybrid composites. Materials & Design 63 (2014) 620-632.

*****